

Controlled Postgrafting of Titanium Chelates for Improved Synthesis of Ti-SBA-15 Epoxidation Catalysts

François Bérubé,[†] Bendaoud Nohair,[†] Freddy Kleitz,^{*,‡} and Serge Kaliaguine^{*,†}

[†]Chemical Engineering Department, Université Laval, Québec, Canada G1 V 0A6 and

[‡]Department of Chemistry, Université Laval, Québec, Canada G1 V 0A6

Received October 2, 2009. Revised Manuscript Received November 27, 2009

A new synthesis procedure that is based on the grafting of titanium alkoxide species chemically modified by acetylacetonate (acac) on the surface of a P123/SBA-15 composite material is proposed to prepare Ti-SBA-15 catalysts and studied by a combination of elemental analysis, Fourier transform infrared spectroscopy (FTIR), solid-state ¹³C (CP) NMR, thermogravimetric analysis (TGA), X-ray diffraction (XRD), diffuse reflectance UV–vis (DR-UV–vis), and N₂ physisorption at –196 °C. In the absence of the acac chelates, the observed formation of anatase TiO₂ onto the surface of the material demonstrates that the coordinating ligand acts as an inhibitor for the crystallization of anatase. Furthermore, FTIR and ²⁹Si NMR results show that the chelated titanium alkoxide precursor interacts strongly with the silanol groups, which, in turn, greatly enhances the dispersion of the titanium species in the mesoporous silica matrix. Moreover, a decrease of the temperature applied for the postgrafting and an increase of both the acac/Ti ratio and pH are shown to favor the retention of titanium on the materials surface without affecting the titanium dispersion. According to the X-ray photoelectron spectroscopy (XPS) results, a maximal titanium content of 13.8% can be well-dispersed on the surface of the mesopores without formation of an excess on the external surface of the solids. However, the results of the DR-UV–vis analyses and the catalytic epoxidation of cyclohexene reveal that the maximal concentration of titanium species in tetrahedral coordination is obtained for materials with a Ti/Si ratio of 5.6%. Even if materials with higher titanium content do not show higher conversion of cyclohexene, they do exhibit remarkably low catalytic deactivation during the recycling tests. A higher hydrothermal stability is suggested as an explanation for the lower deactivation of Ti-SBA-15 at high titanium content.

1. Introduction

Amorphous TiO₂/SiO₂ mixed oxides have been widely used as catalysts for the epoxidation of various alkenes.^{1–3} The use of amorphous SiO₂ as a catalyst support for the dispersion of titanium oxide offers many advantages such as large specific surface area, high thermal stability, and good mechanical strength. In connection with that, the recent discovery of ordered mesoporous silica materials starting with the M41S family⁴ should be viewed as an important breakthrough in the synthesis of Ti-substituted materials. Their large pore sizes (> 2 nm) motivate their use in catalytic reactions involving bulky molecules for which microporous titanium silicalites usually exhibit very low catalytic activity.⁵ Thus, using the surfactant-templating

synthesis pathway, substantial efforts have been deployed to prepare new materials with a variety of mesostructures and pore sizes.^{6–9} In 1998, further progress was achieved by Zhao et al., who synthesized a new family of mesostructured silica materials using nonionic polyalkoxide copolymers as the structure-directing agents.^{10,11} Compared to MCM-41 type materials, this new family of mesoporous materials shows enhanced hydrothermal stability, because of their thicker pore walls (3–6 nm).^{12,13} Since then, efforts have been made to substitute titanium for silicon in the mesostructured SBA-15 silica network, especially via co-condensation reactions of silicon and

*Authors to whom correspondence should be addressed. Tel.: +1 418 656 7812 (F.K.), +1 418 656 2708 (S.K.). Fax: +1 418 656 7916 (F.K.), +1 418 656 3810 (S.K.). E-mail: freddy.kleitz@chm.ulaval.ca (F.K.), serge.kaliaguine@gch.ulaval.ca (S.K.).

(1) Corma, A. *Chem. Rev.* **1997**, *97*, 2373.
(2) Corma, A. *Top. Catal.* **1997**, *4*, 249.
(3) Gallot, J. E.; Kaliaguine, S. *Can. J. Chem. Eng.* **1998**, *76*, 833.
(4) Kresge, C. T.; Leonowicz, M. E.; Roth, W. J.; Vartuli, J. C.; Beck, J. S. *Nature* **1992**, *359*, 710.
(5) Blasco, T.; Corma, A.; Navarro, M. T.; Pérez Pariente, J. J. *Catal.* **1995**, *156*, 65.

(6) Huo, Q. S.; Margolese, D. I.; Ciesla, U.; Demuth, D. G.; Feng, P. Y.; Gier, T. E.; Sieger, P.; Firouzi, A.; Chmelka, B. F.; Schüth, F.; Stucky, G. D. *Chem. Mater.* **1994**, *6*, 1176.
(7) Wan, Y.; Shi, Y. F.; Zhao, D. *Chem. Commun.* **2007**, 897.
(8) Wan, Y.; Zhao, D. *Chem. Rev.* **2007**, *107*, 2821.
(9) Soler-Illia, G. J. A. A.; Sanchez, C.; Lebeau, B.; Patarin, J. *Chem. Rev.* **2002**, *102*, 4093.
(10) Zhao, D.; Feng, J.; Huo, Q.; Melosh, N.; Fredrickson, G. H.; Chmelka, B. F.; Stucky, G. D. *Science* **1998**, *279*, 548.
(11) Zhao, D.; Huo, Q.; Feng, J.; Chmelka, B. F.; Stucky, G. D. *J. Am. Chem. Soc.* **1998**, *120*, 6024.
(12) Khodakov, A. Y.; Zholobenko, V. L.; Bechara, R.; Durant, D. *Microporous Mesoporous Mater.* **2005**, *79*, 29.
(13) Linssen, T.; Cassiers, K.; Cool, P.; Vansant, E. F. *Adv. Colloids Interface Sci.* **2003**, *103*, 121.

titanium precursors.^{14–20} However, this direct synthesis pathway appeared difficult because the initial synthesis conditions involved strong acidic media ($[HCl] = 1.6\text{ M}$), which contribute in maintaining high solubilization of the titanium species. Several methods have then been proposed to improve the incorporation of titanium in mesostructured silicas by such co-condensation of silicon and titanium precursors, namely, by fluoride addition,¹⁶ pH adjustment,¹⁷ or microwave hydrothermal treatment.¹⁸ However, under these conditions, only low loadings of isolated Ti^{4+} into the silica framework could be achieved. Further increase in the titanium content leads to the formation of extraframework anatase TiO_2 species. In our recent studies, different synthesis parameters, e.g., HCl and TEOS concentrations, hydrothermal treatment temperature and time, have been studied systematically over a wide range of Ti/Si molar ratio.^{19,20} These results showed that when the content of titanium, which is substituted into the silica framework, reaches a critical value, anatase TiO_2 clusters form on the material surface. This critical titanium concentration in the solid seemed to be independent of the HCl concentration, but it is strongly influenced by the hydrothermal treatment temperature.¹⁹ Moreover, it was shown that this formation of anatase TiO_2 leads to a marked decrease of the catalytic activity in the epoxidation of cyclohexene.²⁰ A maximal atomic substitution (Ti/Si) of 5.1% was thus obtained for a material that was aged at 35 °C, which is a condition that leads to catalysts with lower hydrothermal stability.¹⁹

Since the formation of an ordered silica mesostructure could only be achieved under specific synthesis conditions (e.g., pH, TEOS and surfactant concentrations, and synthesis temperature), the tuning of the different parameters in the co-condensation-based synthesis of Ti-SBA-15 remains limited. Post-synthesis grafting of a titanium precursor on the surface of mesoporous silica is a viable alternative method for the preparation of titanosilicate materials. In the latter case, the formation of the mesostructure is achieved before the introduction of the titanium precursor on the surface of the materials, and, consequently, it may be performed over a wider range of synthesis conditions. For the same reason, a postsynthesis pathway may also be adapted to a large variety of mesostructured silica (e.g., MCM-41,⁴ SBA-15,¹⁰ KIT-6²¹). Several post-synthesis methods have thus been investigated to disperse titanium alkoxide or titanium chloride on the surface of mesoporous

silica materials.^{22–26} However, the proposed methods sometimes led to the formation of titanium oxide clusters in the channels or on the external surface of the catalysts. Similarly, titanium precursors such as titanocene complexes^{27–29} or titanosilicate molecular precursors³⁰ have also been post-grafted onto amorphous silica materials. There, the use of such chemically modified titanium precursors with organic ligands was shown to result in high titanium dispersion on the silica surface, because of their lower reactivity. However, the high cost of such precursors greatly limits their use.

Other coordinating ligands such as acetic acid, acetylacetonone (acac), and hydrogen peroxide are widely used to stabilize the Ti atoms.^{31,32} The reactivity of these additives with titanium alkoxides could also lead to new molecular precursors that are less prone to hydrolysis.^{33,34} A decreased reactivity in aqueous media, compared to that of the titanium alkoxides, should be beneficial, because it is expected to inhibit extra framework TiO_2 formation on the surface of the silica materials. The method proposed in this study is based on the post-synthesis grafting of a titanium alkoxide, which was modified by acac ligands, on SBA-15 mesoporous silica. Different synthesis parameters (e.g., pH, the acac/Ti molar ratio, and the post-grafting temperature) were systematically studied over a wide range of Ti/Si ratios, to substantiate their influence on the retention of titanium and its relative dispersion on the material surface. The physicochemical properties of the grafted titanosilicate materials were also studied to understand the nature of the interactions between the titanium precursor and the silica surface and to validate the chemical state of the substituted titanium species. Finally, the catalytic activity in the epoxidation of cyclohexene was studied using these grafted materials as catalysts and compared to Ti-SBA-15 synthesized by the co-condensation method. The regenerability of these catalysts was also investigated.

2. Experimental Section

Materials. SBA-15 materials were synthesized using Pluronic P123 (BASF, molecular weight of $M_w = 5800\text{ g/mol}$) as a structure-directing agent and tetraethylorthosilicate (TEOS, 98%, Aldrich) as a silicon source,

- (14) Vinu, A.; Srinivasu, P.; Miyahara, M.; Ariga, K. *J. Phys. Chem. B* **2006**, *110*, 801.
- (15) Chen, Y.; Huang, Y.; Xiu, J.; Han, X.; Bao, X. *Appl. Catal., A* **2004**, *273*, 185.
- (16) Zhang, W. H.; Lu, J.; Han, B.; Li, M.; Xiu, J.; Ying, P.; Li, C. *Chem. Mater.* **2002**, *14*, 3413.
- (17) Wu, S.; Han, Y.; Zou, Y. C.; Song, J. W.; Zhao, L.; Di, Y.; Liu, S. Z.; Xiao, F. S. *Chem. Mater.* **2004**, *16*, 486.
- (18) Newalkar, B. L.; Olanrewaju, J.; Komarneni, S. *Chem. Mater.* **2001**, *13*, 552.
- (19) Bérubé, F.; Kleitz, F.; Kaliaguine, S. *J. Phys. Chem. C* **2008**, *112*, 14403.
- (20) Bérubé, F.; Kleitz, F.; Kaliaguine, S. *J. Mater. Sci.* **2009**, *44*, 6727.
- (21) Kleitz, F.; Choi, S. H.; Ryoo, R. *Chem. Commun.* **2003**, 2136.
- (22) Wu, P.; Iwamoto, M. *J. Chem. Soc. Faraday Trans.* **1998**, *94*, 2871.

- (23) Chiker, F.; Nogier, J. P.; Launay, F.; Bonardet, J. L. *Appl. Catal., A* **2003**, *243*, 309.
- (24) Widenmeyer, M.; Grasser, S.; Köhler, K.; Anwander, R. *Microporous Mesoporous Mater.* **2001**, *44–45*, 327.
- (25) Kim, M. J.; Chang, S. H.; Choi, J. S.; Ahn, W. S. *React. Kinet. Catal. Lett.* **2004**, *82*, 27.
- (26) Luan, Z.; Maes, E. M.; van der Heide, P. A. W.; Zhao, D.; Czernuszewicz, R. S.; Kevan, L. *Chem. Mater.* **1999**, *11*, 3680.
- (27) Ferreira, P.; Gonçalves, I. S.; Kühn, F. E.; Pillinger, M.; Rocha, J.; Santos, A. M.; Thursfield, A. *Eur. J. Inorg. Chem.* **2000**, 551.
- (28) Pérez, Y.; Pérez Quintanilla, D.; Fajardo, M.; Sierra, I.; del Hierro, I. *J. Mol. Catal. A: Chem.* **2007**, *271*, 227.
- (29) Oldroyd, R. D.; Thomas, J. M.; Maschmeyer, T.; MacFaul, P. A.; Snelgrove, D. W.; Ingold, K. U.; Wayner, D. D. M. *Angew. Chem., Int. Ed.* **1996**, *35*, 2787.
- (30) Brutchey, R. L.; Mork, B. V.; Sirbuly, D. J.; Yang, P.; Tilley, T. D. *J. Mol. Catal. A: Chem.* **2005**, *238*, 1.
- (31) Schubert, U. *J. Mater. Chem.* **2005**, *15*, 3701.
- (32) Sanchez, C.; Livage, J.; Henry, M.; Babonneau, F. *J. Non-Cryst. Solids* **1988**, *100*, 65.
- (33) Debsikar, J. C. *J. Mater. Sci.* **1985**, *20*, 44.
- (34) Doeuff, S.; Henry, M.; Sanchez, C.; Livage, J. *J. Non-Cryst. Solids* **1987**, *89*, 206.

following the procedure reported by Choi et al.³⁵ The HCl concentration was lower (0.3 M), compared to the synthesis procedure (1.6 M) initially proposed by Zhao et al.¹⁰ The synthesis was performed with the following initial molar gel composition: 0.99 TEOS/0.54 HCl/0.016 P123/100 H₂O. In a typical synthesis, 6.0 g of Pluronic P123 was dissolved in 114 g of deionized water and 3.5 g of hydrochloric acid (37%) at 35 °C under magnetic stirring. Then, 13.0 g of TEOS was rapidly added to the initial homogeneous solution. The resulting mixture was stirred for 24 h at 35 °C and subsequently hydrothermally treated for an additional 24 h at 100 °C to ensure further framework condensation. The solution containing the solid products was then cooled to room temperature prior to the post-grafting procedure without further treatment. Prior to the titanium addition, the initial solution was stirred at a given temperature and the pH was then adjusted with HCl (37%) or diluted ammonia. For the titanium grafting, tetrapropylorthotitanate (TPOT, 97%, Aldrich) was used as the titanium precursor and acetylacetone (acac, 98%, Aldrich) was used as the ligand. The TPOT and the acac were premixed at a given molar ratio. Twenty grams of anhydrous ethanol was then added, to dilute the previous yellow solution, and the resulting mixture was rapidly added to the initial SBA-15 solution and stirred for 2 h. The solid products were recovered by filtration, washed with 300 mL of anhydrous ethanol, and dried in air at 100 °C for 24 h. Note that this ethanol washing is essential to remove unanchored titanium species from the material surface. Finally, the products were calcined at 550 °C for 3 h to remove the template. The recovered titanosilicate samples are designated using the nomenclature Ti-SBA-15(*w*)-(*x*)-(*y*)-(*z*), where *w* stands for the post-grafting temperature (in °C), *x* is the acac/Ti molar ratio, *y* stands for the pH value, and *z* is the Ti/Si atomic ratio in the recovered solid products (on a percentage basis).

Different series of experiments were conducted to evaluate the effects of these synthesis parameters on the titanium incorporation ratio and coordination number. These different parameters were systematically studied over a wide range of Ti/Si atomic ratio in the initial mixture (0% ≤ Ti/Si ≤ 40%). In a first set of experiments, the effect of the post-grafting temperature (*w* = 5, 25, and 45 °C) was determined. For these samples, the other parameters were kept constant as follows: acac/Ti = 0.79 and pH 0.5. A second set of samples was synthesized to evaluate the effect of the acac/Ti molar ratio (*x* = 0, 0.39, 0.57, 1.57, and 3.15). The other synthetic parameters were kept as follows: *w* = 25 °C and pH 0.5. Finally, a third set of samples was synthesized using different pH (*y* = 0.2, 1, 7, and 10) in the post-grafting solution. For this set of experiments, the other parameters were kept as follows: *w* = 5 °C and acac/Ti = 3.15.

For comparison, Ti-SBA-15 materials were synthesized by co-condensation of TEOS and TPOT using the

procedure described in our recent study.¹⁹ The synthesis was conducted with the following initial molar gel composition: 0.99 TEOS/0.01–0.10 TPOT/0.54 HCl/0.016 P123/100 H₂O. In a typical synthesis, 6.0 g of P123 was dissolved in 114 g of deionized water and 3.5 g of hydrochloric acid (37%) at 35 °C under magnetic stirring. Then, 13.0 g of TEOS and 1.8 g of TPOT were premixed and rapidly added to the initial homogeneous solution to obtain a Ti/Si atomic ratio of 10% in the initial gel. The resulting mixture was stirred for 24 h at 35 °C and subsequently hydrothermally treated for 24 h at 100 °C to ensure further framework condensation. The solid products were recovered by filtration and dried in air at 100 °C for 24 h. Finally, the products were calcined at 550 °C for 3 h to remove the template. Calcined titanosilicate samples synthesized by this direct co-condensation synthesis are designated as Ti-SBA-15(CO)-(z).

Characterization. Wide-angle XRD patterns were recorded using a Siemens Model D5000 diffractometer and Cu K α radiation ($\lambda = 1.5496 \text{ \AA}$). The reference pattern of crystalline anatase was obtained from the Powder Diffraction File 2 (PDF-2) database licensed by the International Center for Diffraction Data (ICDD). Elemental analysis was performed by atomic absorption using a M1100B Perkin–Elmer atomic absorption spectrophotometer. Nitrogen adsorption and desorption isotherms were determined at –196 °C using an ASAP 2010 sorption analyzer. Prior to analysis, samples were outgassed at 80 and 250 °C for as-synthesized and calcined materials, respectively, for 12 h. The pore size distributions were obtained by the non-local density functional theory (NLDFT) method³⁶ and calculated using the Autosorb-1 1.55 software, supplied by Quantachrome Instruments. The NLDFT kernel selected considers sorption of N₂ on silica at –196 °C assuming a cylindrical pore geometry and the model of equilibrium isotherm based on the desorption branch. The total pore volume was calculated at $P/P_0 = 0.95$. Micropore volume was determined from NLDFT cumulative pore volumes estimated for pores < 2 nm (NLDFT kernel of metastable adsorption isotherms). Fourier transform infrared (FTIR) spectra were recorded using a Bio-Rad Model FTS-60 FTIR spectrometer with 1 mg of sample supported on a 100-mg KBr wafer. Diffuse-reflectance UV–vis spectra were recorded using a Varian Cary 500 spectrophotometer that was equipped with a Praying Mantis accessory. A Spectralon reflectance standard was used as a reference. Solid-state ¹³C (CP) NMR spectra were obtained at room temperature on a Bruker Advance 300 MHz spectrometer. The experimental conditions were a recycle delay of 3 s, a number of scans between 14000 and 32000, a contact time of 1 ms, and a ¹H $\pi/2$ pulse of 3.9 μ s. The reference spectra for acetylacetone and isopropanol compounds were obtained from the Spectral Database for Organic Compounds (SDBS). Thermogravimetric analysis (TGA) was conducted under flowing air on a Netzsch STA449C

(35) Choi, M.; Heo, W.; Kleitz, F.; Ryoo, R. *Chem. Commun.* **2003**, 1340.

(36) Ravikovitch, P. I.; Neimark, A. V. *J. Phys. Chem. B* **2001**, *105*, 6817.

Jupiter thermobalance with a heating rate of 10 °C/min. X-ray photoelectron spectroscopy (XPS) spectra were collected on a Kratos Axis-Ultra electron spectrometer (UK) using a monochromatic Al K α X-ray source at a power of 300 W and operated with a base pressure of 5×10^{-10} Torr. Charge compensation was required using a low-energy electron beam perpendicular to the surface of the samples. Survey spectra used for determining the elemental composition were collected at a pass energy of 160 eV. High-resolution spectra of Ti(2p) and O(1s) were collected in conditions giving a nominal energy resolution of 0.5 eV as measured on Ag(3d_{5/2}) (pass energy of 20 eV). High-resolution spectra of C(1s) were collected with pass energy of 40 eV giving a nominal resolution of 0.6 eV. The O(1s) and Ti(2p) binding energies were referenced to the C(1s) line situated at 285.0 eV. The epoxidation of cyclohexene was chosen as the test reaction, and the experimental conditions used were similar to a previously published procedure.³⁷ Cyclohexene (20 mmol), 4 mmol of TBHP (70% in H₂O), 10 mL of acetonitrile, and 0.1 g of catalyst were mixed in a 50-mL round-bottom flask and were heated to 70 °C under stirring for 3 h. The products were analyzed by gas chromatography (Varian CP-3800 gas chromatograph equipped with a Varian CP-SIL capillary column and coupled with a Varian Saturn 2200 mass spectrometer).

3. Results and Discussion

3.1. Post-grafting with a Chelated Titanium Precursor.

To visualize the influence of the different synthesis parameters on the retention of the titanium precursor in the silica material, the Ti/Si atomic ratios of the products recovered (z) were measured, and these data are presented in Figure 1. The different synthesis parameters were studied over a wide range of the titanium precursor initial concentration in the starting synthesis gel. These curves reveal that the interaction between the titanium precursor and the surface of the mesoporous silica is greatly influenced by the synthesis conditions. Titanium precursor retention is clearly favored by an increase of the acac/Ti molar ratio (x). Interestingly, the influence of the acac/Ti atomic ratio on the titanium retention greatly decreased for x values of > 1.57 . In the presence of acac (for $x \geq 0.39$), a steep increase in the titanium-to-silicon atomic ratio (z) is observed at low Ti/Si ratio in the initial gel (Ti/Si $< 5\%$). For higher concentrations of titanium precursor used in the post-grafting solution, the resulting Ti/Si atomic ratios in the recovered materials (z) seem to reach a maximal value, which is dependent on the synthetic conditions. When no acac is used, z values increase exponentially as a function of the Ti/Si atomic ratio used in the post-grafting solution.

Previous studies have demonstrated that the substitution of acac to a titanium alkoxide precursor decreases its reactivity.³⁸ In particular, it was shown that the presence

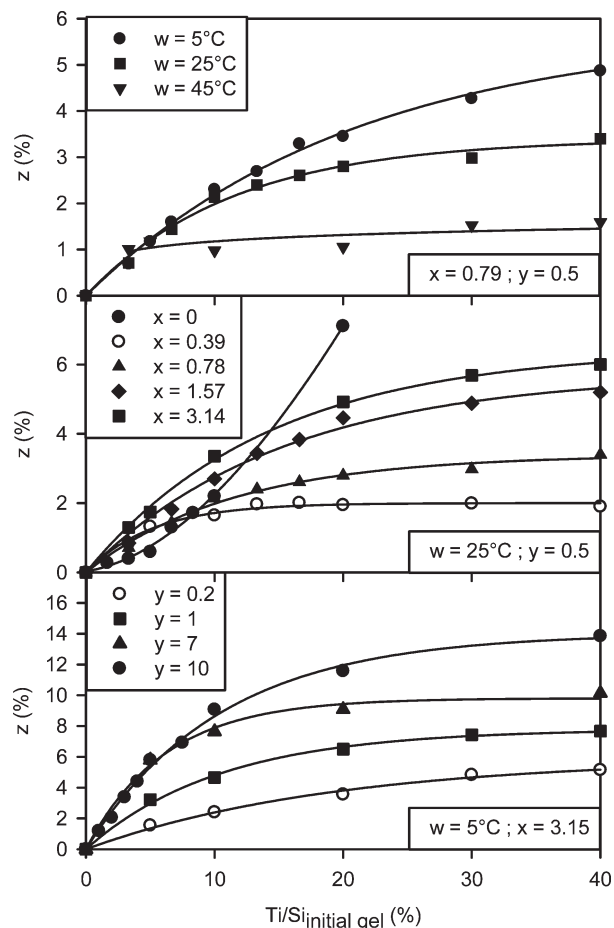


Figure 1. Ti/Si atomic ratio (z) for Ti-SBA-15(w)-(x)-(y) synthesized using different Ti/Si ratios in the initial gel (w stands for temperature (in °C), x stands for the acac/Ti molar ratio, and y stands for pH).

of acetylacetonate in the coordination sphere of titanium inhibits the formation of Ti–O–Ti bonds in aqueous solution.³⁹ Moreover, according to previous studies, two different forms of titanium precursors can be obtained, depending on the acac/Ti ratio used. The substitution of 1 and 2 acac molecules per titanium isopropoxide molecule leads to the formation of dimeric Ti₂(acac)₂(OⁱPr)₆ (1) and monomeric Ti(acac)₂(OⁱPr)₂ (2), respectively (see Scheme 1).^{40,41} Since the reactivity of the modified titanium alkoxide in aqueous media decreases with the number of substituted acac, this could be an explanation for the increase of the titanium retention, as a function of that synthesis parameter.³⁹ Indeed, under the acidic condition used here (pH 0.5), the hydrolysis of the isopropoxy groups of the alkoxide precursor could lead to the protonation of the titanium species thus increasing significantly their solubility. Moreover, a maximal value of 2 acac molecules substituted to the titanium isopropoxide (see Scheme 1) is a possible explanation for the low variation in titanium retention in the silica materials observed for values of $x > 2$. When no acac is used in the post-grafting solution, the hydrolysis rate of the titanium alkoxide is high and the tendency to fill the

(37) Hua, Z.; Bu, W.; Lian, Y.; Chen, H.; Li, L.; Zhang, L.; Li, C.; Shi, J. *J. Mater. Chem.* **2005**, *15*, 661.

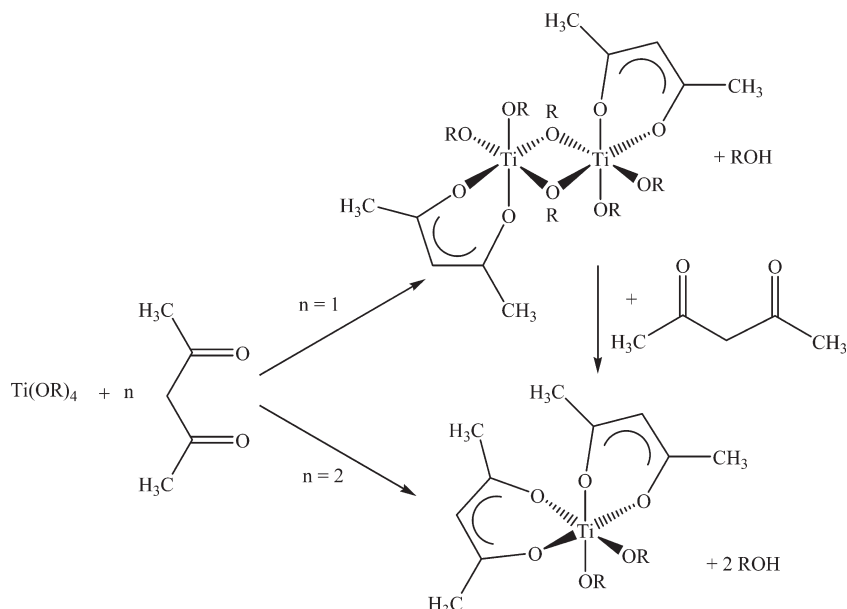
(38) Léaustic, A.; Babonneau, F.; Livage, J. *Chem. Mater.* **1989**, *1*, 248.

(39) Delattre, L.; Babonneau, F. *Chem. Mater.* **1997**, *9*, 2385.

(40) Schmidt, F. *Angew. Chem.* **1952**, *64*, 536.

(41) Yamamoto, A.; Kambara, S. *J. Am. Chem. Soc.* **1957**, *79*, 4344.

Scheme 1. Chemical Modification of Titanium Alkoxide with Acetylacetonate (acac), According to ref 31



coordination sphere of Ti leads to irreversible formation of Ti–O–Ti bonds.⁴² According to our previous study on mesoporous titanasilicate prepared by direct synthesis, such a rapid increase in the titanium retention is observed when the formation of anatase TiO₂ species occurs on the material surface.^{19,20}

Influences of post-grafting temperature and pH on the Ti/Si atomic ratios were also systematically studied. Under acidic conditions (pH < 7), it is shown that the retention of titanium is favored by both a decrease of the temperature of post-grafting and an increase of the pH. These results seem to confirm that the hydrolysis rate and, therefore, the solubility of the modified titanium precursor are indeed higher with increasing temperature and H⁺/Ti ratio.³⁸ Similar results were also obtained by Kim et al. concerning the synthesis of TiO₂ nanoparticles using Ti(acac)₂(OⁱPr)₂ as a titanium source.⁴³ In the synthesis conditions used by these authors, it was found that, for pH > 3, the modified titanium precursor is highly stable and its hydrolysis rate is too low for the formation of TiO₂ nanoparticles. In Figure 1, it is also shown that the Ti/Si atomic ratios in the recovered materials (*z*) continue to increase with higher pH of the solution, even when the H⁺/Ti ratio is essentially negligible (pH ≥ 7). This result suggests that, under these conditions, the interactions between the chelated titanium precursor and the Si–O[−] groups at the surface of the materials are stronger than interactions with the Si–OH and Si–OH₂⁺ groups.

The IR spectra of the calcined titanasilicate materials with different titanium contents are presented in Figure 2. These spectra show three bands—at 800, 1057, and 1228 cm^{−1}—that are associated with Si–O bond-

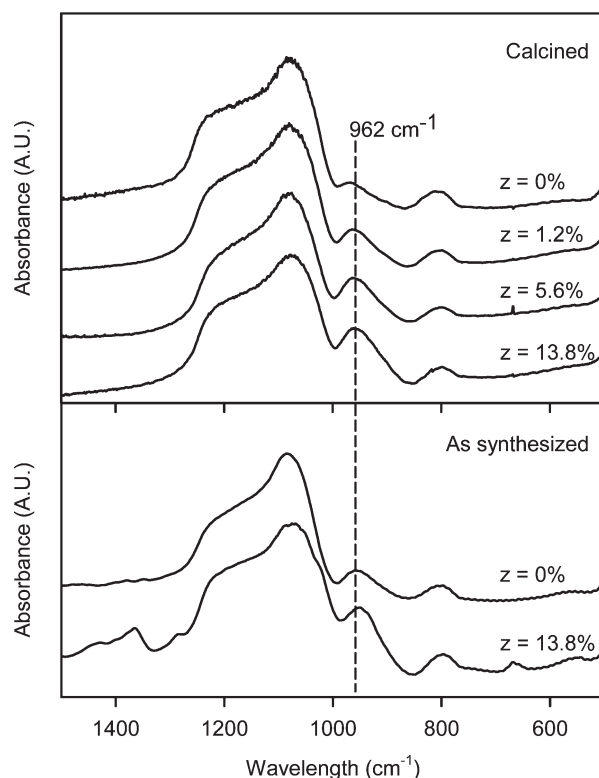


Figure 2. IR spectra of as-synthesized and calcined Ti-SBA-15(5 °C)-(3.15)-(10) for various Ti/Si molar ratios (*z*).

ing.⁴⁴ In addition to these peaks, a band centered at 962 cm^{−1} is generally attributed to the overlapping of vibrations of Ti–O–Si and Si–OH bonds.^{45,46} A comparison of this band with the pure silica sample shows that it is possible to evaluate the amount of Ti–O–Si bonding in

(42) Livage, J.; Henry, M.; Sanchez, C. *Prog. Solid State Chem.* **1988**, *18*, 259.

(43) Kim, Y. T.; Park, Y. S.; Myung, H.; Chae, H. K. *Colloids Surf., A* **2008**, *313–314*, 260.

(44) Eimer, G. A.; Casuscelli, S. G.; Ghione, G. E.; Crivello, M. E.; Herrero, E. R. *Appl. Catal., A* **2006**, *298*, 232.

(45) Guidotti, M.; Ravasio, N.; Psaro, R.; Ferraris, G.; Moretti, J. *J. Catal.* **2003**, *214*, 242.

(46) Wu, P.; Tatsumi, T.; Komatsu, T.; Yashima, T. *Chem. Mater.* **2002**, *14*, 1657.

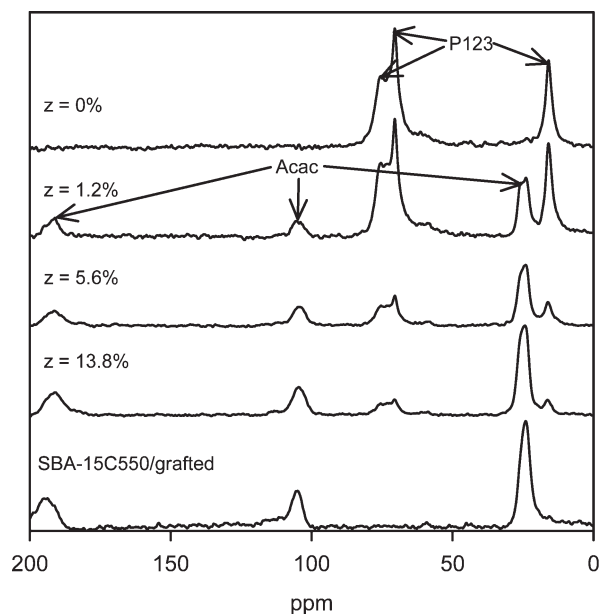


Figure 3. Solid-state ^{13}C (CP) NMR spectra of as-synthesized Ti-SBA-15(5 °C)-(3.15)-(10) with various Ti/Si molar ratios (z). A calcined SBA-15 grafted with acac-modified TPOT and $z = 6.2\%$ is shown for comparison.

the calcined titanosilicate materials. An increase of the intensity of the peaks at 962 cm^{-1} is clearly observed, as a function of the measured Ti/Si ratio in the recovered materials (z). A substantial amount of Ti–O–Si bondings were also observed, indicating that the modified titanium precursor interacts with the silanol groups on the pore surface of the materials. Interestingly, the increase in intensity of this band is very pronounced at low Ti/Si atomic ratio, and it only slightly increases at higher titanium content. To determine whether the formation of these bonds occurs in solution during post-grafting or during the calcination process, IR spectra of as-synthesized SBA-15 and Ti-SBA-15(5 °C)-(3.15)-(10)-(13.8%) materials were collected, as presented in Figure 2. Because the IR spectrum of the sample at $z = 13.8\%$ shows no increase in intensity of the 962 cm^{-1} line, it may be concluded that the linking indeed occurred during the post-grafting process and not during calcination. This is in agreement with the observation made by Delattre et al., who showed that some Ti–O–Si bonds are forming from mixture of $\text{Ti}(\text{acac})_2(\text{O}^i\text{Pr})_2$ and prehydrolyzed solution of TEOS during the preparation of sol–gel-derived $\text{TiO}_2\text{--SiO}_2$ mixed oxides.³⁹ As additional evidence of the Ti–O–Si bond formation, ^{29}Si MAS NMR could provide information about the amount of silanol groups present in the materials. A comparison of the ^{29}Si MAS NMR spectra of the as-synthesized SBA-15 and the Ti-SBA-15(5 °C)-(3.15)-(10)-(13.8%) samples reveals an appreciable decrease ($Q_3/Q_4 = 0.98$ and 0.86 , respectively) in the amount of silanol groups after the grafting of the chelated titanium precursor (see Figure S1 in the Supporting Information), which is consistent with Ti–O–Si bonding formation.

Solid-state ^{13}C (CP) NMR spectra of materials dried at 100 °C are presented in Figure 3. As expected, the ^{13}C

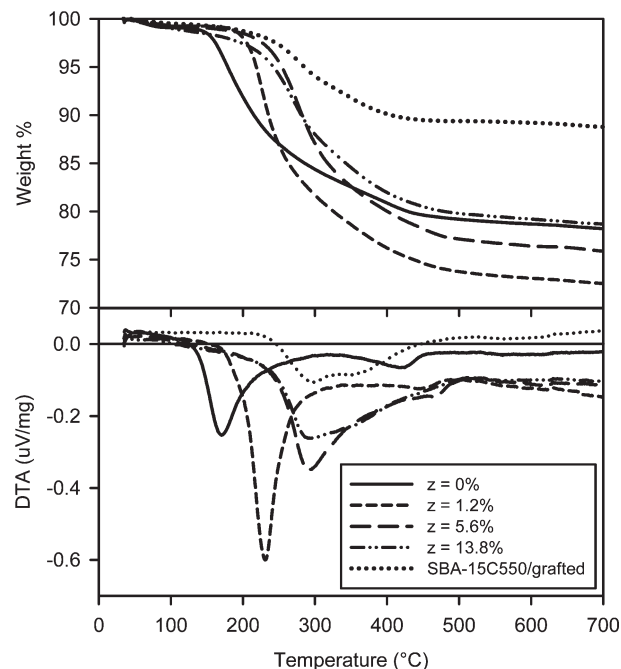


Figure 4. Thermogravimetric analysis (TGA) and differential thermal analysis (DTA) curves of as-synthesized Ti-SBA-15(5 °C)-(3.15)-(10) with various Ti/Si molar ratios (z). Calcined SBA-15 grafted with acac-modified TPOT and $z = 6.2\%$ is shown for comparison.

NMR spectrum of the pure silica sample only shows bands attributed to the P123 block copolymer.^{47,48} For the as-synthesized titanosilicate materials, three lines appear—at 25, 105, and 191 ppm—in addition to the bands associated with the P123. These lines, which are also present for the SBA-15 calcined at 550 °C and then grafted with the acac-modified TPOT, are those of the acac used as the chelating agent. As the Ti/Si ratio increases in the material, the intensity of these lines increases, relative to those of the P123. For the as-synthesized material with a Ti/Si atomic ratio (z) of 13.8% , the carbonaceous species present in the material are mainly constituted of acac. Moreover, no trace of isopropoxy groups was observed via ^{13}C NMR. Such organic species are normally associated with NMR lines at 25 and 64 ppm.

Thermogravimetric analysis (TGA) and differential thermal analysis (DTA) curves of as-synthesized samples with different Ti/Si atomic ratios are presented in Figure 4. The TG profile of the as-synthesized pure silica sample shows a major weight loss at $\sim 175\text{ °C}$, followed by a minor weight loss between 200 °C and 325 °C . These results are in accordance with previous studies and are due to the stepwise removal of the block copolymer from the mesopores and intrawall micropores of the materials.^{49,50} For the materials with a Ti/Si atomic ratio of 1.2% , an increase of the weight loss indicates that the

(47) Yang, C. M.; Zibrowius, B.; Schmidt, W.; Schüth, F. *Chem. Mater.* **2004**, *16*, 2918.

(48) Yang, C. M.; Zibrowius, B.; Schmidt, W.; Schüth, F. *Chem. Mater.* **2003**, *15*, 3739.

(49) Bérubé, F.; Kaliaguine, S. *Microporous Mesoporous Mater.* **2008**, *115*, 469.

(50) Kleitz, F.; Schmidt, W.; Schüth, F. *Microporous Mesoporous Mater.* **2003**, *65*, 1.

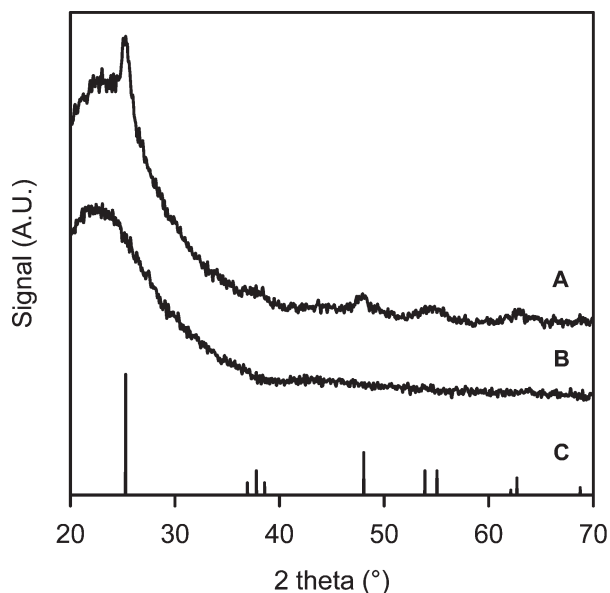


Figure 5. Wide-angle X-ray diffraction (XRD) patterns of calcined Ti-SBA-15(25 °C)-(0)-(0.5)-(7.1%) (pattern A) and Ti-SBA-15(5 °C)-(3.15)-(10)-(13.8%) (pattern B); the reference pattern of anatase TiO₂ is given as spectrum C.

materials. Because the absorption of visible light in the range of 200–400 nm is highly sensitive to the coordination number of the titanium sites and, therefore, to the presence of TiO₂ clusters, this method is widely used to probe the dispersion of titanium in silica materials. A band between 200 nm and 240 nm is generally attributed to a ligand-to-metal charge-transfer transition in isolated TiO₄ units.⁵³ This feature is characteristic of DR-UV-vis spectra of silicalites with low titanium content and is ascribed to tetrahedrally coordinated Ti⁴⁺ species that are incorporated into the silica framework. Bulk TiO₂ in octahedral coordination shows a strong reflectance band centered at 330 nm.^{53–55} Absorption signals between these two bands are attributed to pentacoordinated titanium and/or to small TiO₂ clusters through the quantum size effect.^{56–58}

The effects of three synthesis parameters (temperature, acac/Ti, and pH) on the titanium dispersion are presented in Figure 6. For clarity, the two other parameters were kept constant and the titanium concentrations in the initial gel were carefully chosen to compare materials with similar titanium content (z). In the presence of acac, no substantial change was observed between the DR-UV-vis spectra of materials with similar Ti/Si ratio. When no acac was used ($x = 0$), a weak signal between 300 nm and 400 nm appeared on the DR-UV-vis

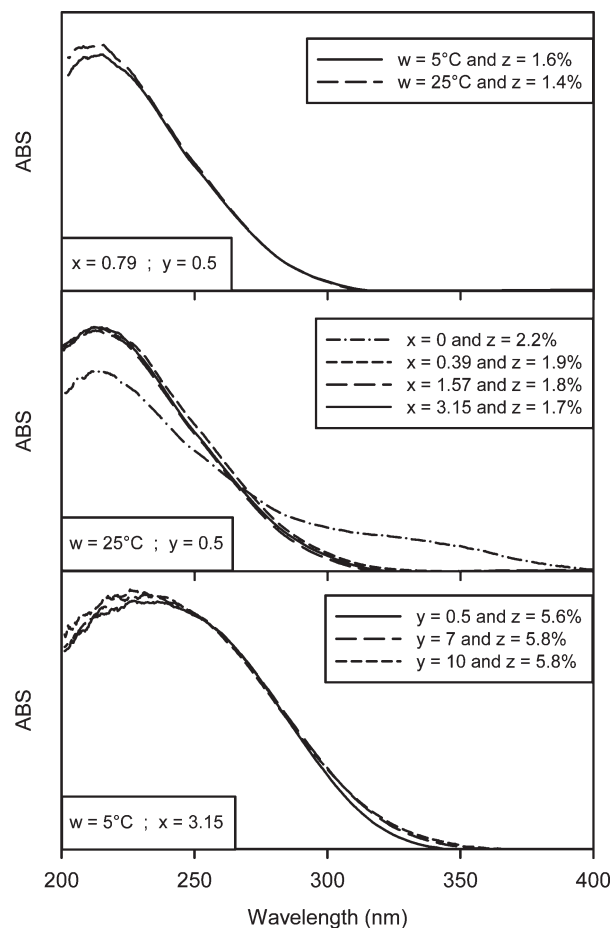


Figure 6. UV-vis diffuse reflectance (DR-UV-vis) spectra of calcined Ti-SBA-15(w)-(x)-(y) with various Ti/Si molar ratios (z); w stands for temperature (in Celsius), x stands for the acac/Ti molar ratio, and y stands for pH.

spectrum and indicates the presence of a small fraction of titanium in octahedral coordination, as corroborated by the XRD data (see Figure 5). The three parameters studied had no effect on the nature of the coordination of the titanium species for acac/Ti ratios of ≥ 0.39 ; therefore, the post-grafting conditions were chosen to maximize the titanium content in the materials. A decreased post-grafting temperature ($w = 5$ °C) with an increased acac/Ti molar ratio ($x = 3.15$) and pH ($y = 10$) were selected to obtain titanasilicate materials with a wide range of possible Ti/Si atomic ratios (see Figure 1). All the Ti-SBA-15 materials discussed below were thus synthesized under these conditions and, therefore, only the Ti/Si atomic ratio of the recovered materials (z) will be reported.

Figure 7 shows the DR-UV-vis spectra of Ti-SBA-15 materials with different Ti/Si atomic ratios. Ti-SBA-15(1.2%) only shows a narrow peak centered at 220 nm indicating that the titanium species present are essentially in tetrahedral coordination. The intensity of the absorption signal at 220 nm increased with the Ti/Si atomic ratio of the material and reached a maximal value for material with $z = 5.6\%$. Moreover, the absorption peak gradually becomes broader extending up to 370 nm for the material with a Ti/Si of 13.8%. This result suggests that small TiO₂

(53) Geobaldo, C. F.; Bordiga, S.; Zecchina, A.; Giamello, E. *Catal. Lett.* **1992**, *16*, 109.

(54) On, D. T.; Le Noc, L.; Bonneviot, L. *Chem. Commun.* **1996**, 299.

(55) On, D. T.; Kapoor, M. P.; Kaliaguine, S. *Chem. Commun.* **1996**, 1161.

(56) Tozzola, G.; Mantegazza, M. A.; Ranghino, G.; Petrini, G.; Bordiga, S.; Ricchiardi, G.; Lamberti, C.; Zulian, R.; Zecchina, A. *J. Catal.* **1998**, *179*, 64.

(57) Geobaldo, F.; Bordiga, S.; Zecchina, A.; Giamello, E.; Leofanti, G.; Petrini, G. *Catal. Lett.* **1992**, *16*, 109.

(58) Deo, G.; Turek, A. M.; Wachs, I. E.; Huybrechts, D. R. C.; Jacobs, P. A. *Zeolites* **1993**, *13*, 365.

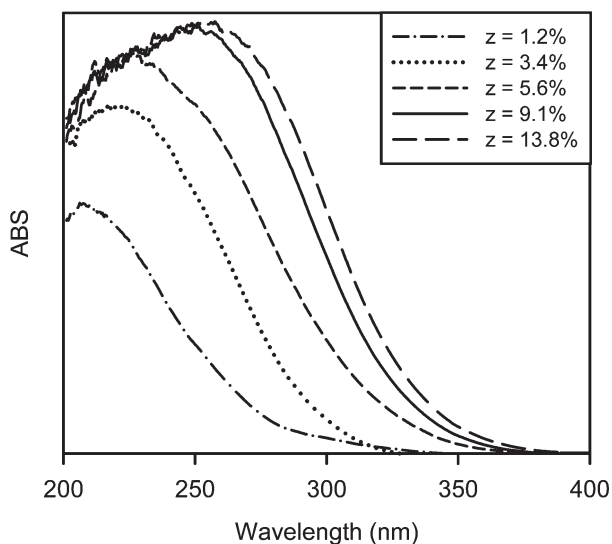


Figure 7. UV-vis diffuse reflectance (DR-UV-vis) spectra of calcined Ti-SBA-15 for various Ti/Si molar ratios (z).

clusters and/or penta-coordinated titanium species appear in these materials. Figure 8A shows O(1s) XPS spectra of Ti-SBA-15 with Ti/Si atomic ratio of 3.1 and 13.8%. The O(1s) XPS spectra of pure silica SBA-15 and anatase TiO₂ are also presented as references and show peaks centered at 533.4 and 530.2 eV, respectively. The O(1s) XPS spectra of materials containing 3.4 and 13.8% show essentially features of a pure silica SBA-15 spectrum and clearly reveal that no titanium in octahedral coordination are present on the external surface of the materials. Moreover, the O(1s) peaks centered at 533.2 and 533.0 eV for materials with Ti/Si atomic ratio of 3.4 and 13.8%, respectively, are slightly shifted toward the lower binding energies. This phenomenon is known for silicon oxides containing substituted transition metal oxides^{59–61} and could be attributed to the presence of Ti–O–Si bonds on the external surface of the materials. The Ti(2p) XPS spectra of Ti-SBA-15 with varying titanium content and that of anatase TiO₂ are shown in Figure 8B. Our previous study indicated that the titanium in tetrahedral coordination substituted to a silica framework displays a line around 460.3 eV and that of extraframework TiO₂ shows a distinct line at 459.0 eV.^{26,62,63} The signals obtained for binding energies between these lines may be assigned to titanium species in intermediate coordination. The Ti(2p_{3/2}) peak of sample with the lower titanium loading ($z = 1.2\%$) shows a large peak centered at 460.7 eV. The titanium species present on the external surface of this sample are tetrahedrally coordinated.

The samples with Ti/Si ratios of 3.4% and 13.8% show a large Ti(2p_{3/2}) peak, centered at 460.3 and 459.7 eV,

respectively, which could be attributed to titanium species in an intermediate coordination state. Generally, the main problem of most post-grafting methods is the presence of an excess of grafted molecules onto the external surface of the materials.²⁶ Therefore, an efficient grafting procedure should lead to a surface density of titanium species grafted on the external surface that does not exceed that of the bulk of the support. This feature was indeed observed for titanosilicate materials prepared by co-condensation when no extra-framework TiO₂ is present on the surface of the materials.²⁰ A comparison between the Ti/Si atomic ratios of Ti-SBA-15(z) samples measured by elemental analysis and by XPS is shown in Figure 9. For samples with $z \leq 3.4\%$, the Ti/Si molar ratios quantified by XPS correspond basically to those measured by elemental analysis. This result indicates that no surface segregation occurs on the external surface of these materials. For samples with higher titanium contents ($z > 3.4\%$), the Ti/Si atomic ratio on the external surface from XPS is lower than the bulk Ti/Si ratio. The absence of any surface segregation of Ti species suggests that the titanium chelates used as titanium precursor can diffuse rather easily through the P123 triblock copolymer soft template. This is likely associated with attractive interactions between the Ti–O–C moieties of the complex and the ether bridges in the ethylene oxide/propylene oxide block copolymer.

Furthermore, as shown by the XRD and DR-UV-vis results, the acac ligands inhibit the formation of anatase TiO₂. Our recent study demonstrated that the tetrahedral TiO₂ species present at the surface of amorphous silica materials were most likely acting as the nuclei for the crystallization of solubilized remaining titanium species.²⁰ Therefore, it is suggested that the reactivity of the titanium species remaining in solution toward the grafted titanium sites is substantially reduced when acac is present in the Ti coordination sphere. These results, which reflect the chemical environment of the titanium on the surface of the silica materials, also show that the present post-grafting method leads preferentially to titanium species that are uniformly dispersed onto the entire surface of the material.

3.3. Textural Properties of Ti-SBA-15 Materials.

Figure S2 in the Supporting Information shows the low-angle XRD pattern for calcined Ti-SBA-15 with a Ti/Si molar ratio of 13.8%. This diffractogram clearly shows three well-resolved diffraction peaks, associated with the (100), (110), and (200) reflections, which is consistent with the two-dimensional (2-D) hexagonal $p6mm$ symmetry. The N₂ adsorption–desorption isotherm of the same material is presented in Figure S3 in the Supporting Information. This material exhibits a type IV isotherm and a H1-type hysteresis loop with steep capillary condensation/evaporation steps, characteristic of high-quality SBA-15 materials synthesized under similar conditions. No pore blocking due to the formation of TiO₂ clusters on the mesopore surface was observed from N₂ desorption at $-196\text{ }^{\circ}\text{C}$. These data confirm that the suggested post-grafting procedure does not alter the

(59) Kim, M.; Jung, S. B.; Kim, M. G.; You, Y. S.; Park, J.; Shin, C.; Seo, G. *Catal. Lett.* **2009**, *129*, 194.

(60) Degirmenci, V.; Erdem, O. F.; Ergum, O.; Yilmaz, A.; Michel, D.; Uner, D. *Top. Catal.* **2008**, *49*, 204.

(61) Zhang, L.; Zhao, Y.; Dai, H.; He, H.; Au, C. T. *Catal. Today* **2008**, *131*, 42.

(62) Kaliaguine, S. *Stud. Surf. Sci. Catal.* **1996**, *102*, 191.

(63) Gao, X.; Bare, S. R.; Fierro, J. L. G.; Banares, M. A.; Wachs, I. E. *J. Phys. Chem. B* **1998**, *102*, 5653.

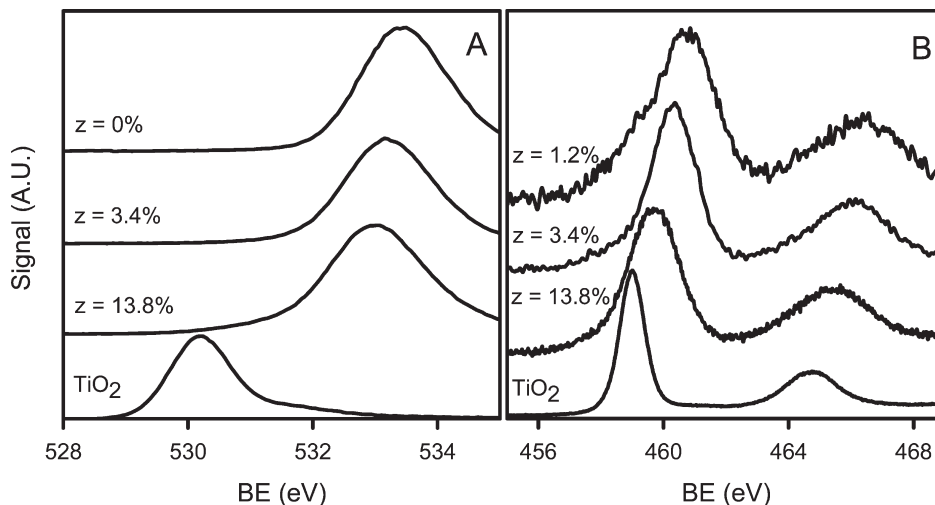


Figure 8. (A) O(1s) and (B) Ti(2p) XPS spectra of calcined Ti-SBA-15 for various Ti/Si molar ratios (z). A reference spectrum of anatase TiO_2 is also given in each panel.

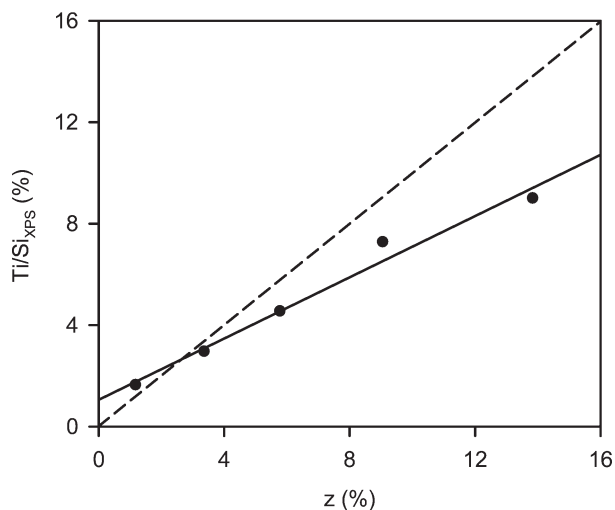


Figure 9. Ti/Si atomic ratio measured by X-ray photoelectron spectroscopy (XPS), as a function of Ti/Si atomic ratio (z) measured by atomic absorption spectroscopy (AAS) obtained for calcined Ti-SBA-15 samples.

structural properties of the materials, even if alkaline conditions are used. Figure 10 shows the evolution of the pore diameter, the total pore volume, and the micropore volume of titanosilicate materials with different Ti/Si atomic ratios (z) before and after calcination at 550 °C. Although an appreciable fraction of residual template is present in the as-synthesized SBA-15 and as-synthesized Ti-SBA-15 materials (see the ^{13}C NMR and TGA results in section 3.1), the N_2 sorption isotherms (not shown) showed steep capillary condensation/evaporation step and large pore diameters and total pore volume. This result indicates that the template which does not interact strongly with the silica walls was easily removed from the mesoporous materials during the ethanol washing. All as-synthesized materials exhibit similar pore diameter excepted for the purely siliceous SBA-15 material which shows a slightly higher pore diameter compared to the titanosilicate samples. Interestingly, the pore diameter of the materials calcined at 550 °C increases with higher Ti/Si atomic ratios. The difference

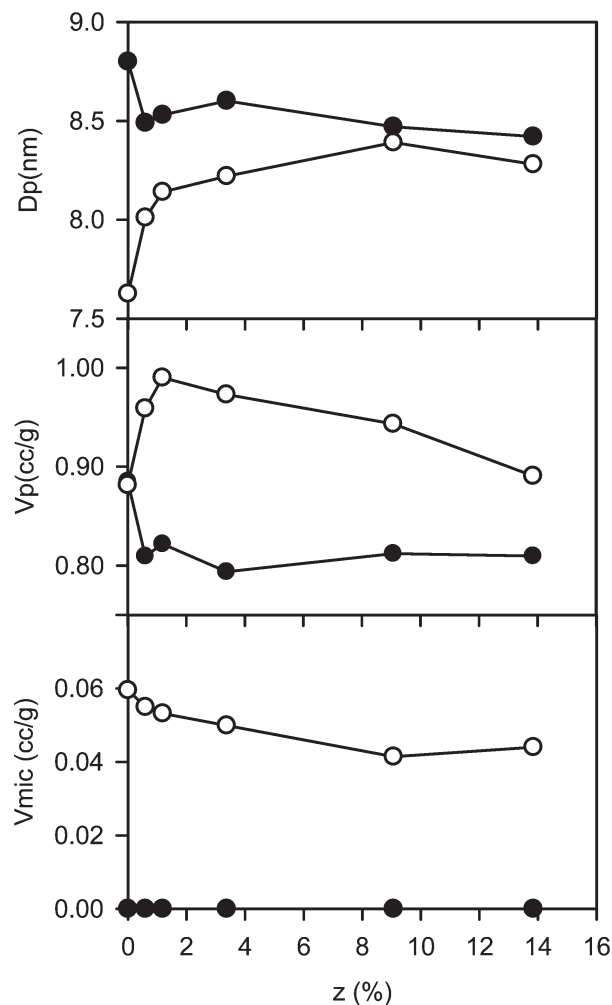


Figure 10. Pore diameters, total pore volumes, and micropore volumes obtained for (●) the as-synthesized and (○) the calcined Ti-SBA-15 for various Ti/Si molar ratios (z).

between the pore sizes of the titanosilicate materials before and after the thermal treatment is thus decreasing as the titanium content is increasing and is almost equal to zero for material with a Ti/Si atomic ratio of 9.1%. These

differences were also observed via low-angle XRD. The lattice parameter (a_0) indeed decreased from 12.8 nm to 11.3 nm for the pure silica SBA-15 sample, while it only decreased from 12.9 nm to 12.0 nm for a Ti-SBA-15 sample with $z = 9.1\%$, before and after the calcination step, respectively. Several studies on the SBA-15 materials have demonstrated that a substantial lattice contraction occurs upon calcination at high temperature.^{11,49,50} This contraction is a consequence of the condensation of network silanol groups present in the as-synthesized material and is thus proportional to the degree of condensation of the silica network. Because the silanol groups react with the titanium precursor during the post-grafting (see section 3.1), a lower lattice contraction during calcination is thus expected, along with an increase in the Ti/Si atomic ratio.

The evolution of the total pore volume as a function of titanium content for as-synthesized materials is rather similar to that of the pore diameter, indicating a correlation between these two structural properties. Higher total pore volumes were measured for calcined materials, probably due to the effect of the residual template present in the as-synthesized materials. For the calcined titanosilicate materials, an increase of the total pore volume was observed up to Ti/Si = 1.2% and is attributed to the steep increase of the pore diameter. For higher titanium content in the materials, the decrease of the specific total pore volume could then be related to the presence of the Ti species in the mesoporous network. Previous reports on SBA-15 materials showed that the hydrophilic part of the block copolymer interacts with the silica species during the formation of the mesostructure.^{49,50,64–66} After removal of the copolymer, this feature would result in the apparition of an intrawall porosity including micropores ($D_p \leq 2$ nm) and small framework mesopores ($D_p > 2$ nm).^{49,66–69} The micropore volumes calculated by the NLDFT method³⁶ are plotted in the lower graph of Figure 10. No micropores were accessible to N₂ for the as-synthesized materials, which suggests that the residual template and/or grafted titanium species are occluded in these framework micropores. After calcination at 550 °C, an appreciable amount of the micropores are liberated and accessible to N₂. A slight decrease of the micropore volume, as a function of titanium content, was nevertheless observed for the calcined samples. This result may be attributed to a partial blocking of this intrawall porosity by the grafted Ti species. In conclusion, these results revealed that the addition of an heteroelement in the silica framework has a drastic effect on the textural

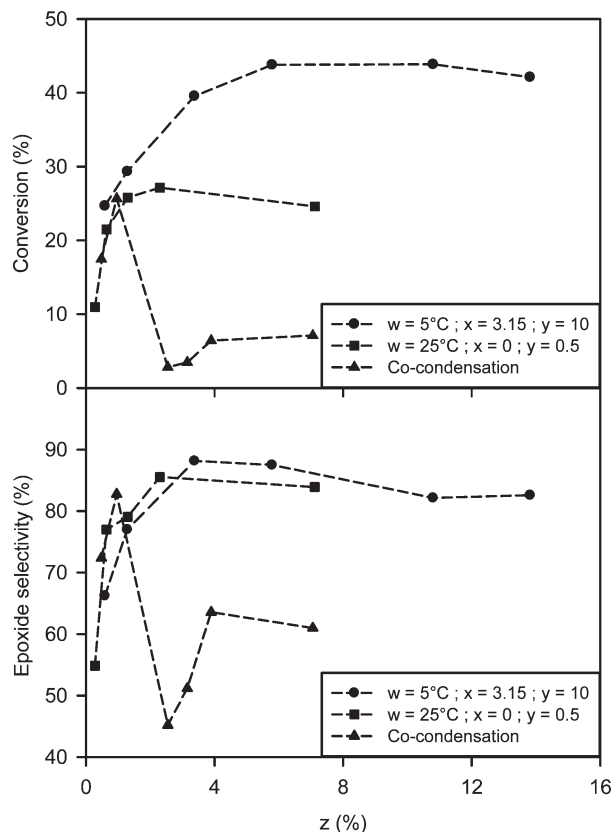


Figure 11. Conversion of cyclohexene and selectivity for cyclohexene oxide obtained on calcined Ti-SBA-15(w)-(x)-(y) with various Ti/Si molar ratios (z); here, w stands for temperature (in Celsius), x stands for the acac/Ti molar ratio, and y stands for pH. A comparison with Ti-SBA-15 synthesized by co-condensation is also given.

properties of the materials after thermal treatment. Moreover, more pronounced modifications of these textural properties were observed for low titanium content (Ti/Si < 3.1%), which suggests that, above a threshold value, the grafted titanium species are not substituted into the framework walls of the materials.

3.4. Catalytic Results. It is well-known that the epoxidation of cyclohexene is only possible over TiO₂-SiO₂ mixed oxides that contain titanium with vacancies in their coordination sphere. The conversion of cyclohexene is thus very sensitive to the coordination environment of the titanium species and has a direct relationship with the concentration of active sites on the material surface. It is important to note that all the materials used as catalysts for cyclohexene epoxidation in this study exhibit similar pore diameters (~8 nm) and specific surface areas (~700 m²/g). The textural properties of these titanosilicate materials are compiled in Table S1 in the Supporting Information. Therefore, these characteristics, in our case, are not a variable in the observed catalytic activity for the cyclohexene conversion. Figure 11 shows the conversion of cyclohexene and the selectivity for the epoxide as a function of the Ti/Si atomic ratio in the catalysts. Three series of catalysts with different titanium loadings were especially compared. By determining the catalytic activity of Ti-SBA-15(5 °C)-(3.15)-(10)-(z) and Ti-SBA-15(25 °C)-(0)-(0.5)-(z) series of materials, it was possible

(64) Ruthstein, S.; Frydman, V.; Goldfarb, D. *J. Phys. Chem. B* **2004**, *108*, 9016.

(65) Ruthstein, S.; Frydman, V.; Kababya, S.; Landau, M.; Goldfarb, D. *J. Phys. Chem. B* **2003**, *107*, 1739.

(66) Galarneau, A.; Cambon, H.; Di Renzo, F.; Ryoo, R.; Choi, M.; Fajula, F. *New J. Chem.* **2003**, *27*, 73.

(67) Ryoo, R.; Ko, C. H.; Kruk, M.; Antochshuk, V.; Jaroniec, M. *J. Phys. Chem. B* **2000**, *104*, 11465.

(68) Liu, Z.; Terasaki, O.; Ohsuna, T.; Hiraga, K.; Shin, H. J.; Ryoo, R. *Chem. Phys. Chem.* **2001**, *4*, 229.

(69) Imperor-Clerc, M.; Davidson, P.; Davidson, A. *J. Am. Chem. Soc.* **2000**, *122*, 11925.

to measure the effect of the acac chelating agent. A third series of catalysts prepared via the direct synthesis (co-condensation) of TPOT and TEOS was also included for comparison. At low Ti/Si atomic ratios in the materials ($z < 1\%$), the conversion of cyclohexene increases steeply as a function of the titanium content, irrespective of the synthesis pathway. It is thus believed that, within this range of titanium content, the titanium species are in tetrahedral coordination and the amount of active sites accessible on the material surface is the only factor that limits the catalytic activity for the epoxidation of cyclohexene. For Ti/Si ratios of $> 1.2\%$, the conversion of cyclohexene decreased drastically for Ti-SBA-15 synthesized via direct synthesis. Our previously reported investigations established that the formation of anatase TiO_2 clusters occurs when a critical titanium concentration is reached in the material.¹⁹ Moreover, it was shown that this critical titanium content is mainly dependent on the aging temperature applied during the synthesis and that a maximal titanium loading that can be well-dispersed at 100 °C into the silica framework is ca. 1%. Since the substituted tetrahedrally coordinated titanium species serve as nuclei for the formation of TiO_2 clusters, this crystallization leads to a decrease in the catalytic activity by reducing the number of accessible active sites.²⁰ When the post-synthesis pathway is performed in the absence of acac ($x = 0$), the conversion of cyclohexene reaches a maximal value of 28% for material with a Ti/Si atomic ratio of 3.1%. A minor decrease in conversion is observed for higher titanium contents, likely because of the formation of anatase TiO_2 (see the XRD results in section 3.2), for the same reason as that previously discussed. Therefore, the addition of acac as an inhibitor for the formation of anatase is expected to have a direct influence on the catalytic activity for cyclohexene epoxidation. A maximal conversion of cyclohexene of 43% is obtained for Ti-SBA-15(5 °C)-(3.15)-(10)-(5.6%), which value is substantially higher than that observed when no acac is used to modify the titanium alkoxide. For catalysts with higher Ti/Si atomic ratios, the conversion of cyclohexene is stable indicating that the addition of Ti does not increase the number of sites active in the epoxidation reaction. Interestingly, the conversion of cyclohexene is directly proportional to the intensity of the band at 220 nm observed on the DR-UV-vis spectra of the materials (see Figure 7), which indicates that only the titanium substituted in tetrahedral coordination is active for the catalytic epoxidation of cyclohexene. In addition to the epoxide, the reaction also leads to the formation of undesirable byproducts. These products are mainly constituted of 2-cyclohexen-1-one and 2-cyclohexen-1-ol.^{37,46} The selectivity for the epoxide was measured and reported in Figure 11. Eimer et al. found, for the epoxidation of cyclohexene over Ti-MCM-41, using H_2O_2 , that the selectivity for epoxide is proportional to the conversion of cyclohexene.⁷⁰ A similar feature is also observed in our

study, because the selectivity toward the epoxide follows a trend resembling that of the cyclohexene conversion, as a function of the titanium loading in the materials. Interestingly, Suh et al. showed that the epoxidation performed over titanosilicate catalysts proceeded through a direct reaction on the active titanium active site in the absence of radicals formation.⁷¹ On the other hand, the cyclohexen-1-ol and cyclohexene-1-one form through allylic oxidation with the radicals originating from the decomposition of the peroxide and promoted by molecular oxygen present in the reaction medium. Moreover, they observed that substantial allylic oxidation occurred in their blank test in the absence of the titanosilicate catalyst. Thus, in contrast to other catalytic systems, an increased selectivity for epoxide is here expected when higher conversions of cyclohexene are obtained because byproduct formation becomes less influenced by the amount of active sites in the reaction medium, compared to the direct epoxidation pathway.

One other relevant characteristic of heterogeneous catalysts is their regenerability. Generally, the epoxidation catalysts synthesized by methods based on post-grafting on the surface of mesoporous silica are more vulnerable to leaching, compared to materials synthesized by co-condensation.⁴⁶ In the latter case, the active sites are dispersed homogeneously in the silica framework, which increases the resistance to leaching.^{70,72} This feature is particularly observed when aqueous solutions of peroxides are used, as is the case in our catalytic study (70% TBHP in H_2O).⁴⁶ Figure 12 shows the cyclohexene conversion and the selectivity of catalysts with different Ti/Si atomic ratios, after three reaction cycles. Ti-SBA-15 synthesized by co-condensation was also compared with the titanosilicate synthesized via the post-grafting pathway. Note that the samples were calcined at 500 °C for 2 h between each reaction cycle. This step is essential for the recovery of the catalysts, because water and/or organic compounds present in the reaction mixture could adsorb on the active titanium sites, increasing their coordination number and deactivating the catalysts. In addition, it was also shown that the reaction conditions can lead to the polymerization of cyclohexene, which could block the active sites of the catalyst. Although the cyclohexene conversion of the initial reaction cycle is quite different for the chosen catalysts, one can see that catalyst deactivation is strongly dependent on the titanium content. The Ti-SBA-15(1.2%) sample showed a dramatic loss of 66% of its conversion after three reaction cycles, whereas the Ti-SBA-15(13.8%) sample only showed a 3% loss. Furthermore, the material synthesized by co-condensation showed a lower deactivation for a similar titanium content, for the reasons discussed previously. It is observed that the active sites of Ti-SBA-15 rich in titanium are more stable against any detrimental effect caused by H_2O present in the reaction mixture. The presence of

(70) Eimer, G. A.; Casuscelli, S. G.; Ghione, G. E.; Crivello, M. E.; Herrero, E. R. *Appl. Catal., A* **2006**, *298*, 232.

(71) Suh, Y. W.; Kim, N. K.; Ahn, W. S.; Rhee, H. K. *J. Mol. Catal. A: Chem.* **2003**, *198*, 309.

(72) Klein, S.; Thorimbert, S.; Maier, W. F. *J. Catal.* **1996**, *163*, 476.

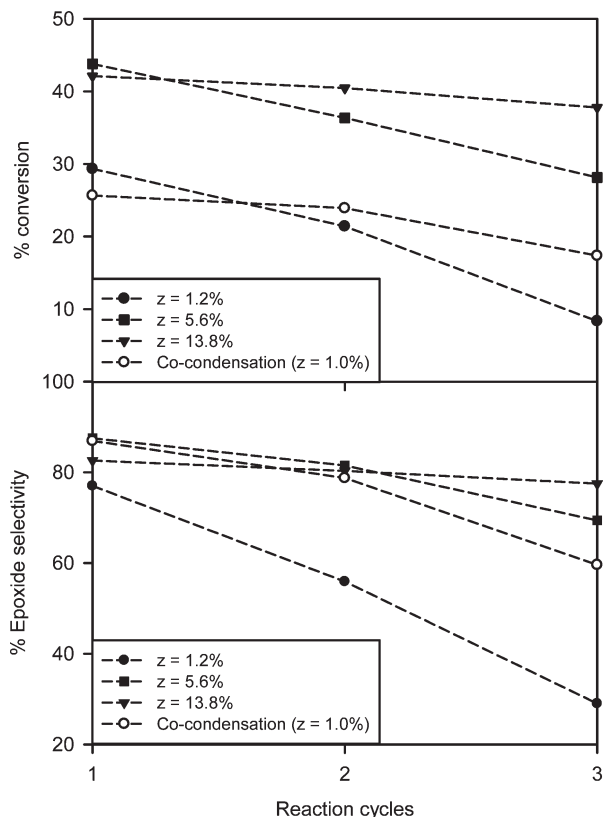


Figure 12. Recycling studies on the calcined Ti-SBA-15 with various Ti/Si molar ratios (z); a comparison with Ti-SBA-15 synthesized by co-condensation is also given.

extra-framework titanium and, therefore, Ti–O–Ti bonds on the surface of the materials could explain this result. Such Ti–O–Ti bonds are more resistant to hydrolysis, compared to Ti–O–Si bonds, and could increase the stability of the active sites on the surface of the materials. Also, rehydroxylation/condensation processes leading to partial structural modifications of the titanosilicate material could not be excluded in the presence of water, and these may result in a reduced accessibility toward the active sites of the materials. On the other hand, an increase in the density of titanium species on the silica surface would stabilize the mesoporous framework, as observed previously, during calcination (see section 3.3). Finally, the evolution of the selectivity for the epoxide on the different reaction cycles follows the same trend as that of the conversion of cyclohexene, as viewed from Figure 11.

4. Conclusions

In summary, this contribution proposes a new method, which is based on the grafting of a titanium alkoxide precursor that is first chemically modified by a chelating agent, namely, acetylacetonate, before being introduced on the surface of P123/SBA-15 composites. It was shown that the presence of acac in the coordination sphere of the titanium species is essential to prevent the formation of anatase TiO₂ on the material surface. Titanium retention in the material was also shown to be strongly dependent on temperature, acac/Ti ratio, and pH of the

post-grafting solution. However, in the presence of acac, the titanium dispersion was proven independent of the above synthesis parameters. Fourier transform infrared (FTIR) experiments strongly suggest that the titanium precursor interacts preferentially with the silanol groups during post-grafting, which leads to the formation of Ti–O–Si bondings. By adjusting the synthesis conditions, Ti-SBA-15 materials with Ti/Si ratios up to 13.8% were obtained. Ultraviolet–visible light diffuse reflectance (DR-UV–vis) and X-ray photoelectron spectroscopy (XPS) experiments also confirmed that the titanium species are well-dispersed on the surface of the mesoporous silica. Comparisons between the physical properties of the parent SBA-15 and those of the titanium grafted SBA-15 indicate that the mild conditions implemented do not alter the initial hexagonal mesostructure. It was moreover established that the presence of grafted titanium species increases the resistance to shrinkage during the calcination process. However, the maximal concentration of titanium species in tetrahedral coordination was obtained for Ti-SBA-15 with a Ti/Si atomic ratio of 5.9%, which is consistent with the higher conversion in the epoxidation of cyclohexene obtained using this material as a catalyst. This conversion of cyclohexene was significantly higher than those measured on Ti-SBA-15 synthesized by co-condensation, proving that this synthesis pathway leads to efficient catalysts for the catalytic epoxidation of alkenes. For materials with higher titanium content (Ti/Si ratios of > 5.9%), the conversion of cyclohexene is stable, indicating that the additional titanium species grafted on the materials are not catalytically active for epoxidation reaction. However, materials with higher amount of grafted titanium species showed a remarkable stability in the catalytic activity during the regeneration process of the catalysts. This feature is especially interesting for further prospects of application of these titanosilicate materials as heterogeneous catalysts.

Acknowledgment. Financial supports from the Natural Sciences and Engineering Research Council of Canada (NSERC) and le Fonds Québécois de la Recherche sur la Nature et les Technologies (FQRNT) are gratefully acknowledged. We thank Professor M. Leclerc from the Department of Chemistry of Université Laval for access to UV–vis spectrometer. We also thank Professor D. Zhao and W. Shen from Fudan University for XRD measurements. F. B. wishes to thank K. Khadrahoui and A. Adnot for help and valuable discussions. F.K. wishes to thank the Canadian Government for the Canada Research Chair on “Functional Nanostructured Materials”.

Supporting Information Available: Table of physicochemical properties of the different Ti-SBA-15 samples used in the catalytic study. Solid-state ²⁹Si MAS NMR data of as-synthesized SBA-15 and Ti-SBA-15-(5 °C)-(3.15)-(10)-(13.8%) materials. XRD pattern of calcined Ti-SBA-15 with a Ti/Si molar ratio (z) of 13.8%. N₂ adsorption–desorption isotherms at –196 °C of calcined Ti-SBA-15 with a Ti/Si molar ratio (z) of 13.8%. (PDF) This material is available free of charge via the Internet at <http://pubs.acs.org>.